ORIGINAL ARTICLE

Customized Fabrication Approach for Hypertrophic Scar Treatment: 3D Printed Fabric Silicone Composite

Lung Chow[1], Kit-Lun Yick[1]*, Mei-Ying Kwan[1], Chun-Fai Yuen[2], Sun-Pui Ng[3], Annie Yu[4], Joanne Yip[1]

[1]Institute of Textiles and Clothing, The Hong Kong Polytechnic University, Hong Kong

[2]University Research Facility in 3D Printing, The Hong Kong Polytechnic University, Hong Kong

[3]Division of Science, Engineering and Health Studies, College of Professional and Continuing Education, The Hong Kong Polytechnic University, Hong Kong

[4]Department of Advanced Fibro Science, Kyoto Institute of Technology, Japan

Abstract: Hypertrophic scars (HS) are considered to be the greatest unmet challenge in wound and burn rehabilitation. The most common treatment for HS is pressure therapy, but pressure garments may not be able to exert adequate pressure onto HS due to the complexity of the human body. However, the development of three-dimensional (3D) scanning and direct digital manufacturing technologies has facilitated the customized placement of additively manufactured silicone gel onto fabric as a component of the pressure therapy garment. This study provides an introduction on a novel and customized fabrication approach to treat HS and discusses the mechanical properties of 3D printed fabric reinforced with a silicone composite. For further demonstration of the suggested HS therapy with customized silicone insert, silicone inserts for the finger webs and HS were additively manufactured onto the fabric. Through the pressure evaluation by Pliance X system, it proved that silicone insert increases the pressure exerted to the HS. Moreover, the mechanical properties of the additively manufactured fabric silicone composites were characterized. The findings suggest that as compared with single viscosity print materials, the adhesive force of the additively manufactured silicone and fabric showed a remarkable improvement of 600% when print materials with different viscosities were applied onto elevated fabric.

Keywords: Three-dimensional printing, Soft material, Textile fabric, Pressure therapy, Hypertrophic scars

1 Introduction

Additive manufacturing, which is known as three-dimensional (3D) printing or rapid prototyping, has been widely adopted in the medical field for fabricating implants, orthoses, and prostheses over the past decade. Recently, the development of 3D printing of flexible and stretchable materials using direct ink writing (DIW) in which the printer extrudes materials out of nozzles have created novel applications in clinical research areas. For example, Zhou *et al*.[1] had produced 3D printed silicone prosthetic noses using DIW and Ahmad Fozi *et al*.[2] had proposed customized silicone facial padding for the hypertrophic scar (HS) management of burn patients using additive manufacturing. The prescribed silicone facial padding takes into consideration patient specific anatomic features which can then exert adequate pressure distribution onto the face, thus improving

scar control for optimum treatment efficacy. Apart from that, Unkovskiy *et al*.[3] also developed a silicone facial prosthesis for rehabilitation treatment based on the direct digital manufacturing (DDM) technique which uses additive manufacturing technologies. DDM is characterized by flexible and lean production process which do not require injection and mold making process[4,5]. It is evident that personalized products can be more readily produced with the use of additive manufacturing to cater to each individual patient based on his/her conditions and needs.

HS is considered to be the greatest unmet challenge in wound and burn rehabilitation. HS is an abnormality in which the epidermis is greatly thickened and collagen is irregularly deposited[6]. As a result, the injured area is thickened, raised, and erythematous in appearance which tremendously affect the quality of life[7]. Apart from cosmetic impairment, functional sequelae can also occur[8]. HS tissue has less elasticity than normal skin tissue, and subsequently, the range of motion of the joints can be limited[9]. The skin is the primary interface between humans and the environment, and therefore is more prone to injury. The most frequent sites for burns in human body part are hand, and when the skin of the hand receives a burn injury and an HS is formed, the range of motion of the fingers decreases[10]. Although the mechanism of treatment process for scars is not well understood, some of the most common rehabilitation treatments for HS in the past decade are the use of pressure therapy and silicone gel sheets[11,12]. Silicone (polysiloxane) is the representative material used for treating HS and has a flexible structure of a backbone chain with alternating oxygen and silicon atoms[13]. Back in early 1980s, Perkins and Davey[14] first suggested the potential of using silicone sheets for treating burn scars. A few years later, silicone in scar treatment was adopted and tested by different researchers[15,16]. The mechanisms of silicone therapy in scars treatment have been suggested by different researchers and the possible suggested effects of silicone include increased skin temperature, hydration of scars, and polarization of scar tissue[17-21]. In practice, pressure therapy is typically used to treat burn victims by providing a continuous pressure of about 25 mmHg to inhibit the growth of HS and encourage its maturation through pressure garments, face masks, casts, splints, or conformers[22-26]. However, the human body has a complex geometry, which means that the pressure exerted onto certain anatomical parts with a concave surface cannot properly inhibits the growth of HS[27]. Therefore, a variety of different materials such as thermal plastic, silicone sheets, or hydrogels are inserted between the skin and the pressure garment to exert adequate pressure onto different body parts and in the case of HS, induce extra pressure onto the scar for effective treatment[17,28]. However, these additional inserted materials like silicone sheets are usually larger in size than the HS[17]. The unnecessary pressure and coverage will cause excessive sweating, pruritus or even contact dermatitis of the healthy skin next to the HS[17,29]. Another limitation of pressure therapy is material deterioration with gradual loss of pressure with use. During the application of pressure therapy, repeated joint movements stretch the pressure therapy garment which reduces the elasticity of the fabric[30]. As a result, the pressure therapy garment has to be replaced or adjusted after a period of time to ensure adequate pressure performance and effectively treat HS to facilitate recovery. To improve the treatment process, different types of therapies can be collectively applied at the same time[31]. Li-Tsang *et al*.[32] concluded that the integration of pressure and silicone gel sheeting therapy has a positive and better effect in reducing scar thickness than the conventional use of pressure garments.

In this study, we propose an innovative and customized fabrication approach with the use of 3D scanning and DDM of silicone technology. Medical-grade silicone is extruded through a nozzle directly onto the fabric based on 3D scanned data to provide an accurately sized insertion material which would optimize the pressure delivery. Hence, adequate pressure is induced onto the HS by the printed silicone gel with the benefit of silicone treatment while the individual variations of the anatomical features are also taken into consideration. This combined therapy which integrates pressure and

silicone sheet therapy provides a more effective result in reducing the scar thickness. Since the amount of pressure induced by a pressure garment also depends on the mechanical properties of the fabric, the influence of 3D printed silicone gel on the mechanical behavior and tension decay after repeated extensions of the warp-knitted fabric used for pressure therapy garments was also determined to provide new insights into the wider application of 3D printing, such as clinical applications, flexible electronics and wearable products, and development of soft robotics and actuators.

2 Materials and methods

2.1 3D modeling and fabrication

The geometry of the hands of a patient with HS was obtained using a structured light handheld 3D scanner (Artec Eva, Luxembourg). After scanning was completed, the scanned images were registered using Artec Studio 13. The registered point cloud data were then imported into processing software (Materialise Magics) and converted into 3D mesh models for the fabrication process. The models for printing were based on the amount of redness and protrusion of the HS and point cloud data. After obtaining the desired models, the model meshes and coordinates were adjusted with reference to the required orientation and dimensions of silicone gel, as well as the method of garment prototyping before the fabrication process took place.

Warp knitted fabric made of a blend of nylon (83%) and spandex (17%) with a total weight of 165 g/m^2 and 0.226 mm in thickness, which is the typical type of fabric used for pressure therapy garment, was applied as the reinforcement of the composite. In consideration of the adhesion of the fabric and printed silicone gel, two print mixtures with two different viscosities were prepared. A biocompatible silicone elastomer (SILBIONE® RTV 4410 1:1 A and B) was mixed with 0.2 and 2 wt% of a silicone thickener (THI-VEX™), respectively, and degassed for 3D printing onto the fabric. The 3D printing was carried out using a 3D-printer (3D-Bioplotter® Manufacturer Series) and the settings and printing toolpaths are shown in **Table 1** and **Figure 1,** respectively.

To characterize the mechanical properties of the printed composite, the samples were additively manufactured at 20 × 100 × 2.24 mm for cyclic tensile testing, the size stated in ASTM D5169 Standard Test Method for Shear Strength (Dynamic Method) of Hook and Loop Touch Fasteners and ASTM D638-14 Standard Test Method for Tensile Properties of Plastics (Type V specimens) to test the adhesive force and tensile properties, respectively. The adhesive behavior of three different samples was evaluated. The 3D printing parameters of the samples are listed in **Table 2**. Note that, pigment was added into the print mixture for visualization and surface morphology investigation purposes, and no pigment was added to the samples for the mechanical characterization. Furthermore, the surface morphology of the ASTM D5169 samples was observed using an optical microscope.

Table 1. Parameters of different print mixtures of 3D-Printing process.

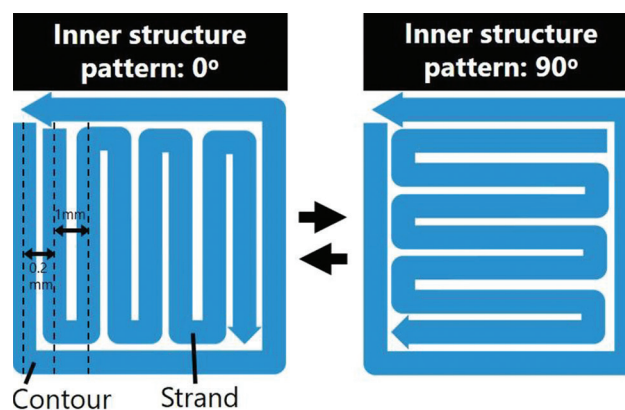| Print mixture	SILBIONE® RTV 4410 1:1 A and B+0/0.2/.2.0 wt% THI-VEXTM
Nozzle diameter (mm)	0.4
Printing speed (mm/s)	20
Build Platform temperature (°C)	70
Head temperature (°C)	0
Path width (mm)	~0.6
Inner structure pattern(°)	0,90

3D: Three-dimensional

Figure 1. 3D printing toolpath.

Table 2. 3D printing parameters of the test samples.

Testing	ASTM D5169		Cyclic tensile testing	ASTM D638-14 Type V	
Sample code	0.2 wt%_Thickener_ 0.4 mm	2 wt%_Thickener	Fabric silicone composite	Silicone	Fabric silicone composite
Print mixture for the first layer	SILBIONE® RTV 4410 1:1 A and B+0.2 wt% THI-VEX™	SILBIONE® RTV 4410 1:1 A and B+2 wt% THI-VEX™	SILBIONE® RTV 4410 1:1 A and B+2 wt% THI-VEX™	SILBIONE® RTV 4410 1:1 A and B+2 wt% THI-VEX™	SILBIONE® RTV 4410 1:1 A and B+0.2 wt% THI-VEX™
Print mixture for the others layer	SILBIONE®+2 wt% THI-VEX™				
Distance between the build platform and fabric (mm)	0.4	0 (Direct contact)	0.4	0 (Direct contact)	0.4
No. of layer	10	10	8	3	3
No. of sample	5	5	1	3	3

3D: Three-dimensional

2.2 Mechanical characterization

The tensile properties of the fabricated composite and silicone gel were determined using the Instron 5566 universal mechanical test frame in accordance with ASTM D638-14 (Type V specimen) at a speed of 100 mm/min. The viscosity of silicone print mixtures with different concentration of thickener was tested by a rotational viscosity meter at 0°C. The adhesion between the printed silicone and fabric was tested in accordance with ASTM D5169 at a speed of 305 mm/min. The dynamic stress-strain behavior of the composite with repeated extension and recovery cycles was measured to determine the loss of fabric tension which would result in pressure degradation. A total of 3000 tensile cycles were carried out with the Instron 5566 for the fabric and fabric silicone composite samples, and the tensile values were recorded. The parameters were a strain of 50%, gauge length of 40 mm, and speed of 500 mm/min.

2.3 Pressure garment production and pressure characterization

The patterns of pressure garment were developed based on the scanned hand geometry data and three reduction factors (namely, 0, 10%, and 20% reduction in the width of the patterns), respectively. A total of six pressure garments were custom-made and their corresponding amount of pressure dosage applied onto the HS with or absence of silicone insert was measured and analyzed. The fabric applied was same as the one for silicone composite printing.

The exerted pressure to HS was evaluated by NOVEL Pliance X system. The sensor was inserted between the pressure garment and the skin while the hand was kept in a static relax position on a table for 20 s for static pressure recording.

3 Results and discussion

3.1 Scanned geometry and structure of fabricated composites

First, the models for 3D printing (**Figure 2A** and **B**) were created based on the 3D- scanned geometry of the hand to allow optimum fit of the insertion
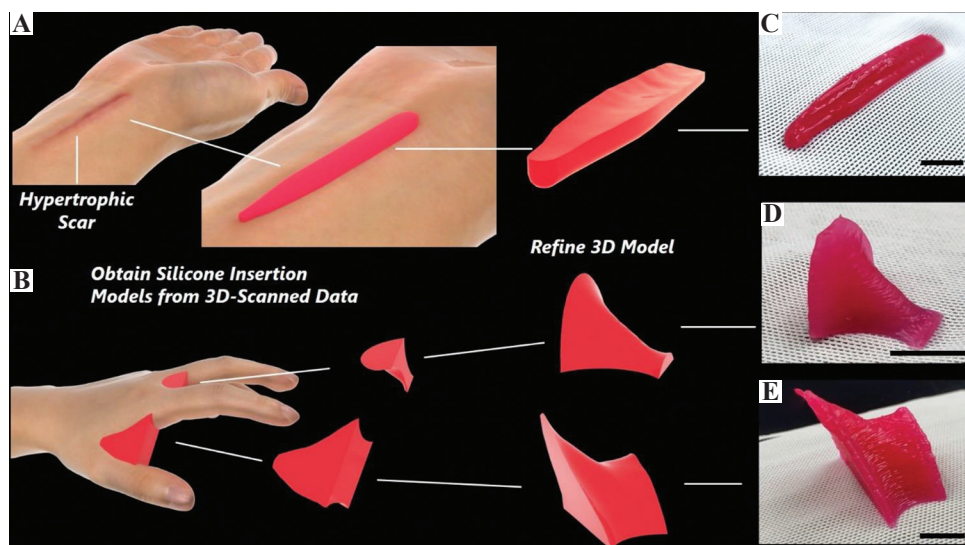
Figure 2. Schematic of workflow and production process of additively manufactured silicone inserts: Three-dimensional (3D) scanned geometry of (A) hypertrophic scars (HS) with refined insertion models and (B) hand with refined web insertion models. Photo of 3D printed: (C) Insertion for the HS; (D) and (E) web insertion for webspace between second and third digits; Scale bar: 10 mm.

materials. After that, the 3D models were refined, and the model orientation was adjusted for printing. Finally, the 3D models were imported into the 3D-printer (3D-Bioplotter® Manufacturer Series) for the additive manufacturing process. **Figure 2C-E** is the photo of the silicone inserts which can function as orthoses to prevent web space contractures during therapy[17,33]. When comparing the traditional manual insert material production and the 3D printing process, the 3D printing production process minimizes human errors in orthosis design and achieves a reliable and repeatable geometry of inserts. Once the silicone insert was 3D printed on fabric, it could be sewn as a part of the pressure garment to increase pressure onto the specific body region and prevent the distal migration of scars. For silicone gel sheet therapy, the planar shape of silicone gel sheet is usually larger than the size of HS regardless of the 3D body shapes and curvatures, thus leading to displacements, ill-fitting, and discomfort during the treatment, **Figure 3A** and **B**. When comparing with silicone gel sheet therapy, the accurate geometric shape of the printed silicone inserts prevents negative impacts such as excessive sweating, pruritus, and contact dermatitis of the healthy skin next to the HS, **Figure 3C**. Moreover, the silicone inserts can administer the right amount of pressure at the interface between the scar and garment for effective scar reduction by combining and reinforcing the pressure, hydration, and static electricity stimulation together[17].

3.2 Mechanical performance of fabricated composites

3.2.1 Adhesion force

To achieve an additive manufactured product with high resolution, a print silicone mixture with high viscosity needs to be used. However, high viscosity silicone mixtures do not easily diffuse through fabric; hence, resulted in poor shear strength of the 3D printed silicone and fabric. To prevent the pressure garment fabric and 3D printed silicone inserts from separating during wearing, a multi-material printing approach was adopted to improve the force of the adhesion. The schematic of this approach is shown in **Figure 4**. During the printing process, a lower viscosity (around 7400 Mpa·s) silicone mixture was used in the first printed layer, while a higher viscosity (around 1,080,000 Mpa·s) silicone mixture was used in the other printed layers. The viscosity curve of the silicone print mixtures with different thickener contents at 0°C, which is the temperature of the print head, as a

Figure 3. Differences between the suggested hypertrophic scars (HS) treatment with customized silicone insert and traditional silicone gel sheet therapy: (A) Photograph of the HS; (B) Demonstration of tropical silicone gel sheet therapy; (C) Demonstration of suggested HS treatment with customized silicone insert.
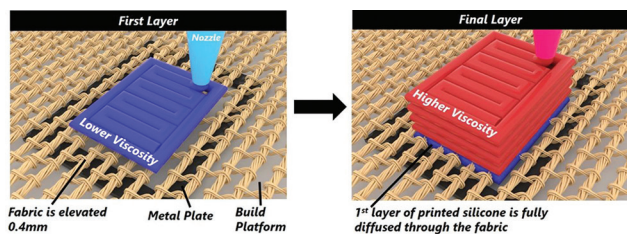

Figure 4. Schematic of multi-material approach on elevated fabric.

reference shown in **Figure 5A** for various materials printing on fabric. Theoretically, lower viscosity of print mixture is easier to diffuse through the fabric. However, too low viscosity print mixture may cause the undesirable diffusion and migration of the silicone mixture, adversely affecting the control of the printing process and the ultimate size and shape of the printed composite. **Figure 5B** and **C** shows the problem of extremely low viscosity print mixture during printing. The first layer of printed silicone mixture in **Figure 5B** without thickener which spread along the print platform before curing and causing improper size of printed material. Therefore, 0.2 wt% thickener was added to increase the viscosity of mixture from around 2300 to 7400 Mpa·s for the first layer of printing (**Figure 5C**). To further improve the adhesion between the fabric and silicone, a metal plate was placed between the fabric and the build platform that the fabric specimen was elevated to accommodate the deposition of silicone mixture. At the same time, the temperature of the build platform was set to 70ºC to facilitate the curing of the 3D printed silicone to create a stable base for the above layers.

The adhesion force of the samples was determined using ASTM D5169, which is used to examine the adhesion of 3D printed materials and textiles[34]. The schematic diagram of ASTM D5169 is shown in **Figure 5D**. Images of the 3D printing process of ASTM D5169 samples for mechanical characterization and the printed sample are shown in **Figure 5E** and **F**.

The maximum shearing force of the 0.2 wt%_Thickener _0.4 mm elevated sample is around 60 N which is a 600% improvement in comparison to the result of 2 wt%_Thickener sample; **Figure 5G** and **H**. When comparing the 0.2 wt%_Thickener _0.4 mm and 0.2 wt%_Thickener samples, the elevation of fabric increases around 50% of maximum shearing force. To investigate the surface morphology of the samples, blue and red pigments were added to the print mixtures of the first and other layers, respectively. It is shown in **Figure 5Ii** and **Iii** that more of the silicone mixture has diffused through the fabric in 0.2 wt%_Thickener_0.4 mm sample when compared to 0.2 wt%_Thickener sample which demonstrates the effect of the elevating the layer of fabric. For the 0.2 wt%_Thickener_0.4 mm elevated sample, due to the elevation of fabric, extra capacity is provided for the diffusion of the silicone mixture. As a result, a sandwich structure composite was fabricated, which consists of two silicone outer skins and a fabric core structure. The sandwich structure of sample increases the contact surface area between the silicone and fabric and, at the same time, creates mechanical barriers that interlock the porous fabric. Consequently, the adhesive force of this sample is significantly higher since tearing of silicone is required to separate the silicone from the fabric. In contrast, the silicone mixture with high viscosity 2 wt%_Thickener sample did not diffuse through the fabric or absorbed by the yarn,
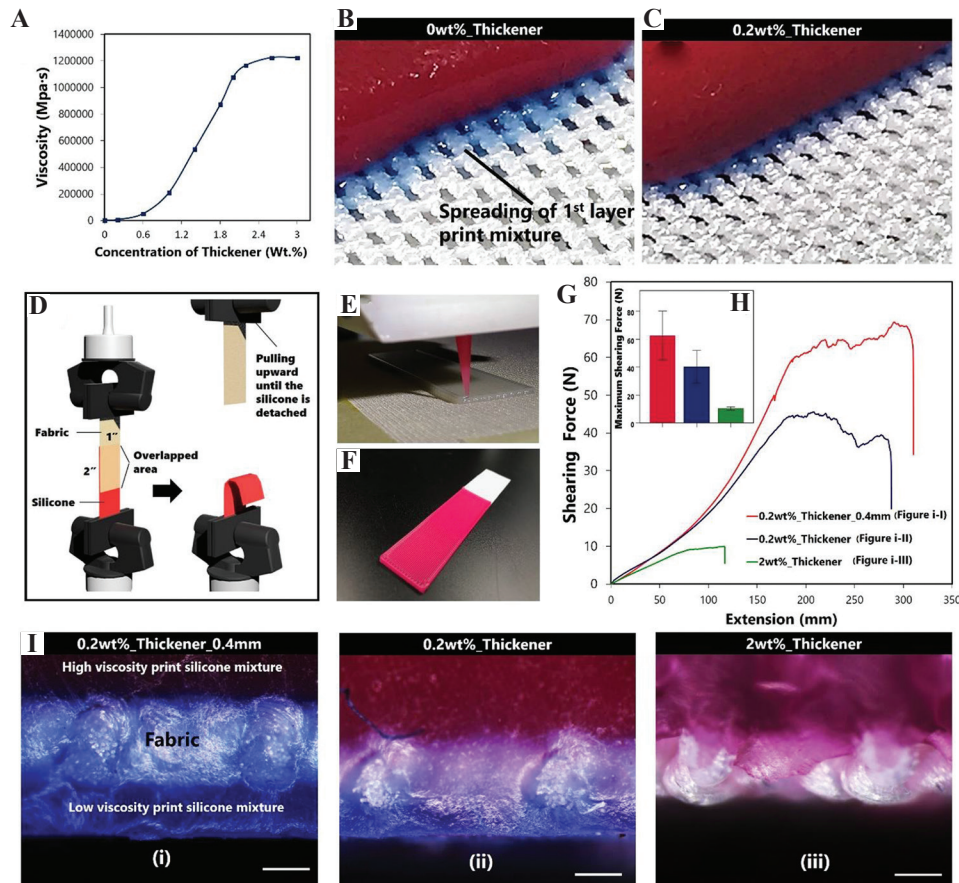
Figure 5. Investigation of adhesion of three-dimensional (3D) printed silicone on fabric: (A) Viscosity curve of the silicone print mixtures with different thickener contents; (B) and (C) demonstration of the problem of extremely low viscosity of print mixture for first layer printing, (D) schematic of ASTM D5169; (E) image of 3D printing process of ASTM D5169; (F) image of a ASTM D5169 sample; (G) plotted shearing forces versus extension; (H) maximum shearing force comparison; (I) cross-sectional observation of (i) 0.2 wt%_Thickener_0.4 mm sample, (ii) 0.2 wt%_Thickener sample, and (iii) 2 wt%_Thickener sample; Scale bar: 200 μm.

as shown in **Figure 5Iiii**. Therefore, its shear strength is mainly contributed by the adhesion and friction of the silicone and fabric and result in much lower shearing strength than the other samples.

The proposed printing approach here shows a dramatic improvement of adhesion (600% in shear strength) between the fabric and silicone which demonstrates its potential for customizing any type of application, such as wearable electronics, soft robotics, engineered foot insoles, and orthotic bracewear.

Although the use of the proposed multi-material approach on elevated fabric improves the adhesion of the printed material and fabric, the size of the print model should be considered. As the fabric has high flexibility, the distance between the build platform and fabric can be reduced due to gravity, especially in the middle of the elevated area if a large print model is required. As a result, the adhesion between the fabric and silicone can be reduced. Furthermore, the shape of the model for printing can be affected due to the caving-in of the fabric.

3.2.2 Tensile properties

The durability of a material is a key element of pressure therapy because undependable materials

may create significant challenges when determining the pattern size of garments. Conventional materials for pressure therapy garments such as nylon/spandex blended warp knitted fabrics will deform and lose their elasticity, which reduce pressure delivery and the treatment effectiveness[30,35]. Silicone, however, has excellent resilience that the material is able to withstand repeated functional loading without dimensional changes[35]. The stress of the composite consists of the fabric and silicone is lower than the fabric itself due to the lower strength of the used silicone when comparing with the materials of fabric. **Figure 6A** is the comparison of tensile properties of the fabric and fabric silicone composite before and after 3000 cycles of tensile testing. In terms of the deformation and change in the Young's modulus, the fabric silicone composite showed less reduced tensile strength after 3000 cycles of testing. More
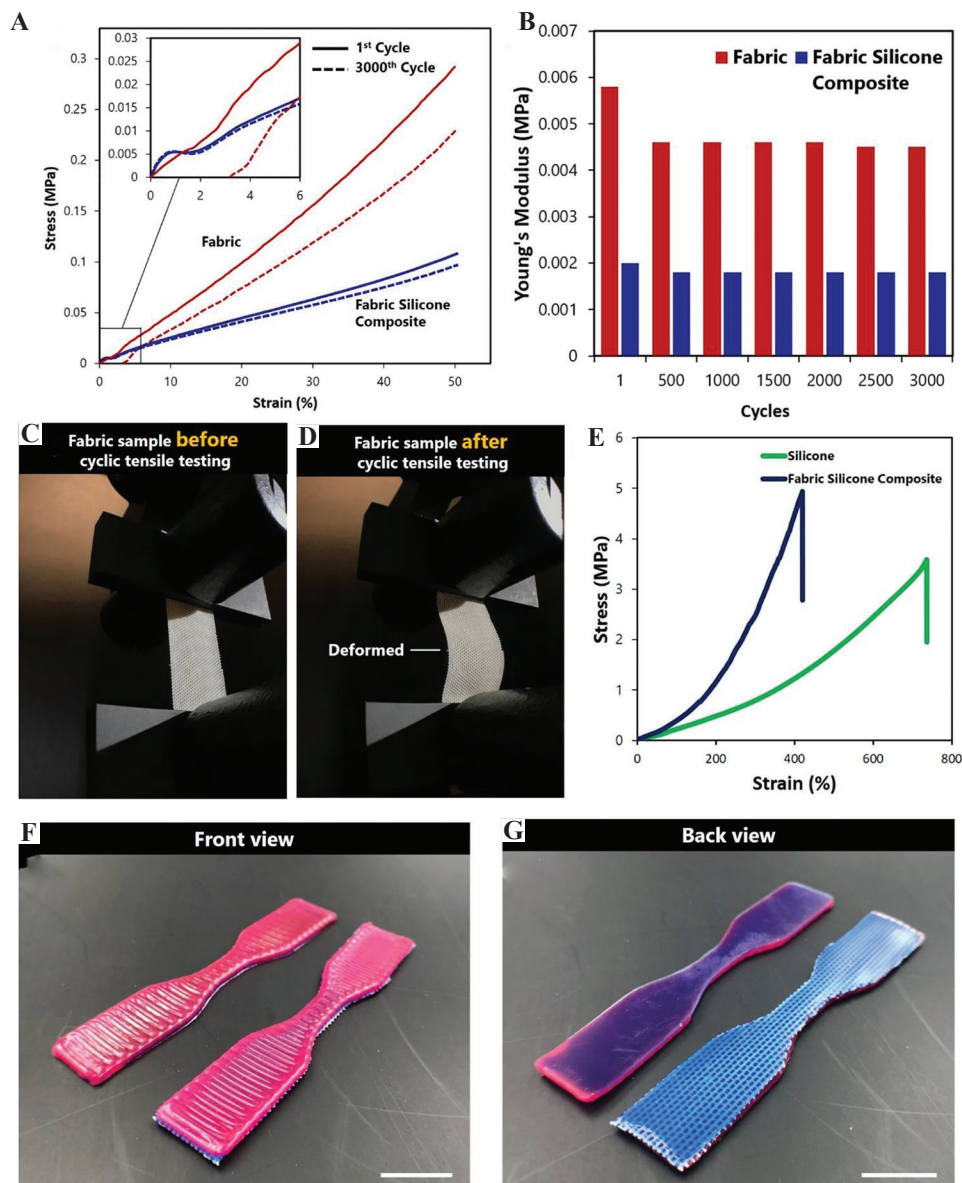

Figure 6. Investigation of deterioration of material and tensile properties: (A) Stress-strain curves of fabric and fabric silicone composite samples before and after cyclic tensile testing; (B) Young's modulus of fabric and fabric silicone composite samples; (C) and (D) fabric sample before and after cyclic tensile testing; (E) stress-strain curves of fabric and fabric silicone composite samples; (F) and (G) front and back view of ASTM D638 samples; scale bar: 10 mm.

detailed changes in the Young's modulus for every 500 cycles are shown in **Figure 6B**. The percentage of decline in the Young's modulus of the fabric silicone composite sample was 55% less than that of the fabric sample after 3000 cycles of testing. There was approximately 3% deformation that can be found in the fabric sample after 3000 cycles of testing while no deformation can be found for the fabric silicone composite. The images in **Figure 6C** and **D** show the deformation of the fabric after 3000 cycles of testing. The reason of the fabric deformation after tensile cycles could be explained by the friction between the fiber and yarn in the complex interlooping fabric structure. When the tensile force is applied onto the fabric, the fabric is extended and the loop is deformed in the vertical direction. Once the force is released, the yarn and fiber fail to recover to their original shapes due to the high friction induced by the large contact surface area between the fibers and yarns. The experimental result evidently proved that the fabricated fabric silicone composite has a better durability in shape recovery and mechanical properties after extension and recovery since the silicone matrix stabilizes the structure of the fabric which results in higher elasticity. As a result, the pressure garment is able to exert adequate pressure onto the skin of patients during wear to provide better pressure therapy treatment. Apart from material fatigue, we have also shown the tensile properties of the fabric silicone composite and silicone samples using ASTM D638; **Figure 6E**. The fabricated samples are shown in **Figure 6F** and **G**. The fabric reinforcement approach improved the strength of the 3D printed silicone. Our example shows the means of modifying the mechanical behavior of 3D printed soft material using a fabric reinforcement method in a flexible way. Another advantage of the fabric reinforcement
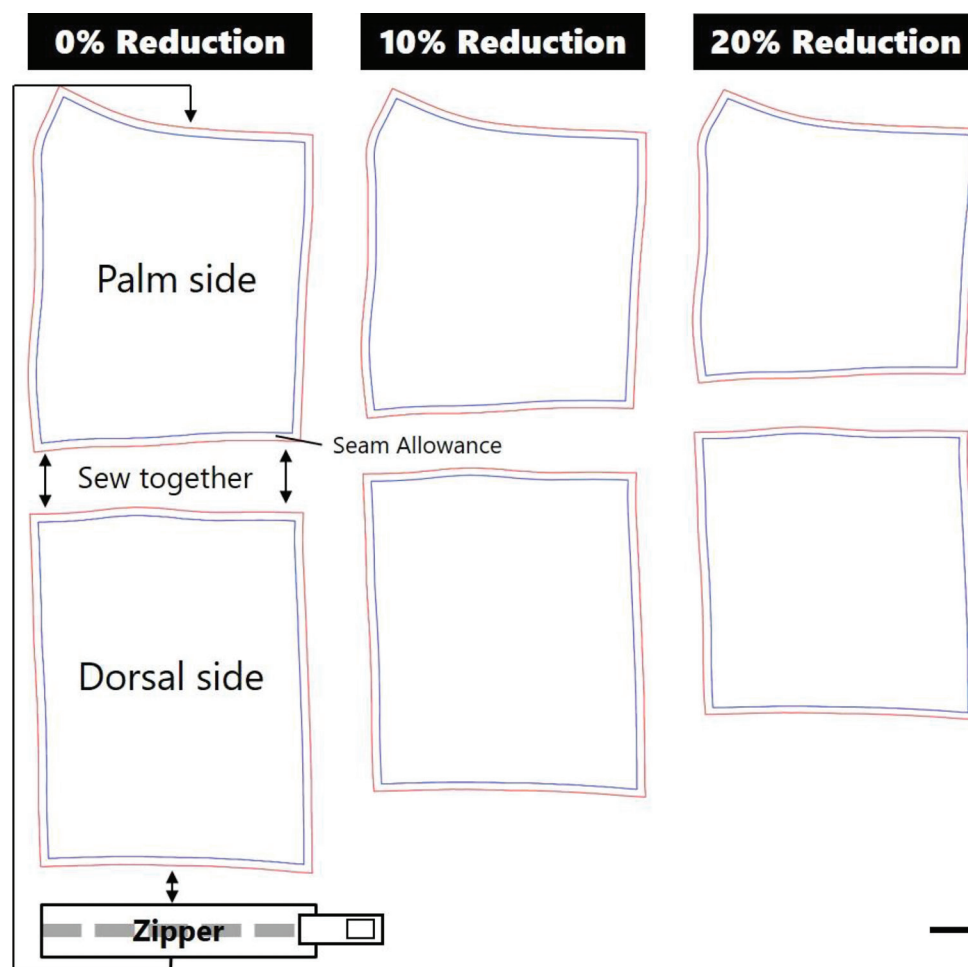

Figure 7. Patterns of the pressure garment and the assembly method; scale bar: 10 mm.
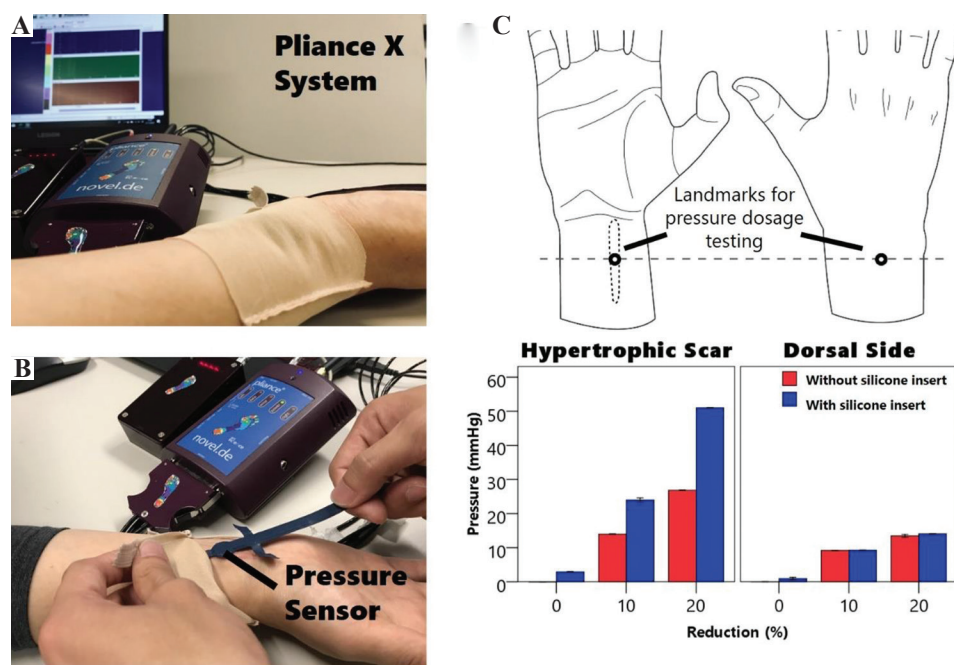
Figure 8. Pressure dosage evaluation by Pliance X System: (A) The overview and setup of Pliance X System; (B) insertion of the pressure sensor between the hypertrophic scars and pressure garment; (C) the differences of pressure dosage between traditional pressure therapy and the suggested customized silicone insert pressure therapy.

approach is that sewing of soft material can be realized due to the core fabric structure. The reinforced soft material can be stitched with various materials such as smart and shape memory materials, or optical fibers which are convenient for developing smart textiles, and wearable and electronic devices.

3.3 Effect of silicone insert on pressure delivery

Figure 7 shows the patterns of the pressure garment in different reduction factors and the assembly method. In our study, the NOVEL Pliance X system was adopted for measuring the interface pressure generated by the pressure garment which had been evaluated and validated for accuracy by different researchers[36,37]. The system was characterized by the slim size of sensor which is <10 mm in diameter and 1 mm in thickness. **Figure 8A** shows the overview of Pliance X system and **Figure 8B** demonstrates the process of inserting the sensor between the pressure garment and the HS. Due to the tiny size of the sensor, it can be inserted under the pressure garment easily. The landmarks for pressure dosage testing and the

result can be referred to **Figure 8C**. The result clearly proved the silicone insert can specifically increase the interfacial pressure between the insert and the HS in all garment size (reduction) conditions, while its influence of pressure on other body regions (dorsal side) was somewhat subtle. The result indicates that 10% size reduced garment with silicone insert could exert around 25 mmHg pressure to the HS to encourage their maturation and inhibit their growth. Although the 20% size reduced garment could also exert around 25 mmHg pressure to the HS, the patients had major difficulties to put on the garment and fasten the zipper which may adversely affect the practical use of pressure garment with high risk of injuries to the skin. It may induce excessive pressures onto the healthy skin, leading to limitations of movements and discomfort to the patient. In this study, the integrated 3D printed silicone insert and pressure therapy can exert the specific and adequate amount of pressure onto different body parts to effectively treat HS, thus benefiting burn patients toward a quicker recovery.

4 Conclusion

In this study, we have introduced an innovative and customized fabrication approach for HS treatment by utilizing 3D scanning and DDM of silicone technology. The 3D printed fabric silicone composite is customized based on the geometry of the HS and hand obtained from a 3D scanning process, and as a component of a pressure therapy garment. To demonstrate the application of DDM of silicone technology to pressure therapy gloves, inserts for the finger webs and HS have been additively manufactured.

The results of the mechanical characterization show that our new additively manufactured fabric silicone composite is less likely to deform with better durability as opposed to the conventional warp knitted fabric used for pressure therapy garments that experiences a gradual loss of fabric tension and pressure after repeated wear. Through the pressure characterization, the result also indicates our suggested that HS therapy can effectively and specifically exert adequate pressure to the scar location, while preserving the wearing comfort of non-scar body parts.

It is anticipated that the approach proposed in this study would not be limited to pressure garment therapy but opens up another means of customization where products can be designed for specific purposes with individual variations such as anatomically engineered foot insoles and orthotic bracewear. The experimental results also demonstrate the possibility of modifying the mechanical behavior of 3D printed soft material using the fabric reinforcement approach which creates new insights for clinical applications, flexible electronics, and wearable products, as well as in the development of soft robotics and actuators.

Acknowledgments

Disclosure statement

No potential conflicts of interest were reported by the authors.

References

1. Zhou L, Gao Q, Fu J, *et al.*, 2019, Multi-Material 3D Printing of Highly Stretchable Silicone Elastomer. *ACS Appl Mater Interfaces*, 11(26):23573–83. DOI: 10.1021/acsami.9b04873.

2. Fozi MA, Salleh MN, Ismail KA, 2019, Development of 3D-printed Customized Facial Padding for Burn Patients. *Rapid Prototyp J*, 25(1):55–61. DOI: 10.1108/rpj-09-2017-0179.

3. Unkovskiy A, Spintzyk S, Brom J, *et al.*, 2018, Direct 3D Printing of Silicone Facial Prostheses: A Preliminary Experience in Digital Workflow. *J Prosthet Dent*, 120(2):303–8. DOI: 10.1016/j.prosdent.2017.11.007.

4. Gibson I, 2015, In: Rosen DW, Stucker B, editors. Additive Manufacturing Technologies: 3D Printing, Rapid Prototyping, and Direct Digital Manufacturing. 2nd ed. Springer, New York. DOI: 10.1007/978-1-4939-2113-3_16.

5. Bibb R, 2015, In: Dand E, Paterson A, editors. Medical Modelling: The Application of Advanced Design and Rapid Prototyping Techniques in Medicine. 2nd ed. Woodhead Publishing, Cambridge.

6. Li-Tsang CW, Feng B, Huang L, *et al.*, 2015, A Histological Study on the Effect of Pressure Therapy on the Activities of Myofibroblasts and Keratinocytes in Hypertrophic Scar Tissues After Burn. *Burns*, 41(5):1008–16. DOI: 10.1016/j.burns.2014.11.017.

7. Yu A, Yick KL, 2018, Compression and stretch fit garments. In: Engineering of High-Performance Textiles. Woodhead Publishing, Sawston, United Kingdom. pp. 279-303. DOI: 10.1016/b978-0-08-101273-4.00011-1.

8. Cho YS, Jeon JH, Hong A, *et al.*, 2014, The Effect of Burn Rehabilitation Massage Therapy on Hypertrophic Scar after Burn: A Randomized Controlled Trial. *Burns*, 40(8):1513–20. DOI: 10.1016/j.burns.2014.02.005.

9. Dewey WS, Richard RL, Parry IS, 2011, Positioning, Splinting, and Contracture Management. *Phys Med Rehabil Clin*, 22(2):229–47.

10. Kwan P, Hori K, Ding J, *et al.*, 2009, Scar and Contracture: Biological Principles. *Hand Clin*, 25(4):511–28. DOI: 10.1016/j.hcl.2009.06.007.

11. Carney BC, Liu Z, Alkhalil A, *et al.*, 2017, Elastin is Differentially Regulated by Pressure Therapy in a Porcine

Model of Hypertrophic Scar. *J Burn Care Res*, 38(1):28–35. DOI: 10.1097/bcr.0000000000000413.

12. Wei Y, Wang Y, Zhang M, *et al.*, 2018, The Application of 3D-printed Transparent Facemask for Facial Scar Management and its Biomechanical Rationale. *Burns*, 44(2):453–61. DOI: 10.1016/j.burns.2017.08.006.

13. Liravi Fand Toyserkani E, 2018, Additive manufacturing of silicone structures: A review and prospective. *Addit Manufact*, 24:232–42. DOI: 10.1016/j.addma.2018.10.002.

14. Perkins K, Davey R, Wallis K, 1983, Silicone Gel: A New Treatment for Burn Scars and Contractures. *Burns*, 9(3):201–4. DOI: 10.1016/0305-4179(83)90039-6.

15. Mercer NGS, 1989, Silicone Gel in the Treatment of Keloid Scars. *Plast Surg Nurs*, 9(4):162.

16. Quinn K, Evans J, Courtney J, *et al.*, 1985, Non-pressure Treatment of Hypertrophic Scars. *Burns*, 12(2):102–8. DOI: 10.1016/0305-4179(85)90035-x.

17. Van den Kerckhove E, Stappaerts K, Boeckx W, *et al.*, 2001, Silicones in the Rehabilitation of Burns: A Review and Overview. *Burns*, 27(3):205–14. DOI: 10.1016/s0305-4179(00)00102-9.

18. Gilman TH, 2003, Silicone Sheet for Treatment and Prevention of Hypertrophic Scar: A New Proposal for the Mechanism of Efficacy. *Wound Repair Regen*, 11(3):235–6. DOI: 10.1046/j.1524-475x.2003.11313.x.

19. Ko WJ, Na YC, Suh BS, *et al.*, 2013, The Effects of Topical Agent (Kelo-cote or contractubex) Massage on the Thickness of Post-burn Scar Tissue Formed in Rats. *Arch Plast Surg*, 40(6):697–704. DOI: 10.5999/aps.2013.40.6.697.

20. Di Rocco G, Gentile A, Antonini A, *et al.*, 2011, Enhanced Healing of Diabetic Wounds by Topical Administration of Adipose Tissue-Derived Stromal Cells Overexpressing Stromal-Derived Factor-1: Biodistribution and Engraftment Analysis by Bioluminescent Imaging. *Stem Cells Int*, 2011:304562. DOI: 10.4061/2011/304562.

21. Berman B, Perez OA, Konda S, *et al.*, 2007, A Review of the Biologic Effects, Clinical Efficacy, and Safety of Silicone Elastomer Sheeting for Hypertrophic and Keloid Scar Treatment and Management. Malden, USA. pp. 1291–303. DOI: 10.1111/j.1524-4725.2007.33280.x.

22. Bosworth C, 2002, Burn Trauma: Management and Nursing Care. 2nd ed. Whurr, London.

23. Macintyre L, Gilmartin S, Rae M, 2007, The Impact of Design Variables and Aftercare Regime on the Long-term Performance of Pressure Garments. *J Burn Care Res*, 28(5):725–33. DOI: 10.1097/bcr.0b013e318148c999.

24. Leung P, Ng M, 1980, Pressure Treatment for Hypertrophic Scars Resulting from Burns. *Burns*, 6(4):244–50. DOI: 10.1016/s0305-4179(80)80007-6.

25. Rivers E, Strate R, Solem L, 1979, The Transparent Face Mask. *Am J Occup Ther*, 33(2):108–13.

26. Staley MJ, Richard RL, 1997, Use of Pressure to Treat Hypertrophic Burn Scars. *Adv Wound Care*, 10(3):44-6.

27. Yu A, Yick KL, Ng SP, *et al.*, 2016, Orthopaedic Textile Inserts for Pressure Treatment of Hypertrophic Scars. *Textile Res J*, 86(14):1549–62. DOI: 10.1177/0040517515573409.

28. Pendleton H, Schultz-Krohn W, 2018, Pedretti's Occupational Therapy: Practice Skills for Physical Dysfunction. 8th ed. Elsevier Health Sciences, Amsterdam, Netherlands.

29. Uslu AA, Sürücü AA, Korkmaz AM, *et al.*, 2019, Acquired Localized Hypertrichosis Following Pressure Garment and/or Silicone Therapy in Burn Patients. *Ann Plast Surg*, 82(2):158–61. DOI: 10.1097/sap.0000000000001686.

30. Yu A, Yick KL, Ng SP, *et al.*, 2013, Prediction of Fabric Tension and Pressure Decay for the Development of Pressure Therapy Gloves. *Textile Res J*, 83(3):269–87. DOI: 10.1177/0040517512456757.

31. Juckett G, Hartman-Adams H, 2009, Management of Keloids and Hypertrophic Scars. *Am Fam Phys*, 80(3):253–60.

32. Li-Tsang CW, Zheng YP, Lau JC, 2010, A Randomized Clinical Trial to Study the Effect of Silicone Gel Dressing and Pressure Therapy on Posttraumatic Hypertrophic Scars. *J Burn Care Res*, 31(3):448–57. DOI: 10.1097/bcr.0b013e3181db52a7.

33. Kamal RM, Khalaf MM, Elshazely A, *et al.*, 2016, Dynamic Splint Versus Static Splint and Active Range of Motion in Treatment of Post Burn Hand Contracture. *Int J PharmTech Res*, 9(6):75–83.

34. Narula A, Pastore CM, Schmelzeisen D, *et al.*, 2018, Effect of Knit and Print Parameters on Peel Strength of Hybrid 3-D Printed Textiles. *J Textiles Fibrous Mater*, 1:1–5. DOI: 10.1177/2515221117749251.

35. Hearle JW, 2008, In: Morton WE, editor. Physical Properties of Textile Fibres. 4th ed. Elsevier Science, Burlington.

36. Lai CH, Li-Tsang CW, 2009, Validation of the Pliance X System in Measuring Interface Pressure Generated by Pressure Garment. *Burns*, 35(6):845–51. DOI: 10.1016/j.burns.2008.09.013.

37. Wiseman J, Simons M, Kimble R, *et al.*, 2018, Reliability and Clinical Utility of the Pliance X for Measuring Pressure at the Interface of Pressure Garments and Burn Scars in Children. *Burns*, 44(7):1820–8. DOI: 10.1016/j.burns.2018.05.002.